LETTER

doi:10.1038/nature09860

A Raf–induced allosteric transition of KSR stimulates phosphorylation of MEK

Damian F. Brennan[1]*, Arvin C. Dar[2]*, Nicholas T. Hertz[2], William C. H. Chao[1], Alma L. Burlingame[3], Kevan M. Shokat[2] & David Barford[1]

In metazoans, the Ras–Raf–MEK (mitogen-activated protein-kinase kinase)–ERK (extracellular signal-regulated kinase) signalling pathway relays extracellular stimuli to elicit changes in cellular function and gene expression. Aberrant activation of this pathway through oncogenic mutations is responsible for a large proportion of human cancer. Kinase suppressor of Ras (KSR)[1–3] functions as an essential scaffolding protein to coordinate the assembly of Raf–MEK–ERK complexes[4,5]. Here we integrate structural and biochemical studies to understand how KSR promotes stimulatory Raf phosphorylation of MEK (refs 6, 7). We show, from the crystal structure of the kinase domain of human KSR2 (KSR2(KD)) in complex with rabbit MEK1, that interactions between KSR2(KD) and MEK1 are mediated by their respective activation segments and C-lobe αG helices. Analogous to BRAF (refs 8, 9), KSR2 self-associates through a side-to-side interface involving Arg 718, a residue identified in a genetic screen as a suppressor of Ras signalling[1–3]. ATP is bound to the KSR2(KD) catalytic site, and we demonstrate KSR2 kinase activity towards MEK1 by *in vitro* assays and chemical genetics. In the KSR2(KD)–MEK1 complex, the activation segments of both kinases are mutually constrained, and KSR2 adopts an inactive conformation. BRAF allosterically stimulates the kinase activity of KSR2, which is dependent on formation of a side-to-side KSR2–BRAF heterodimer. Furthermore, KSR2–BRAF heterodimerization results in an increase of BRAF-induced MEK phosphorylation via the KSR2-mediated relay of a signal from BRAF to release the activation segment of MEK for phosphorylation. We propose that KSR interacts with a regulatory Raf molecule in *cis* to induce a conformational switch of MEK, facilitating MEK's phosphorylation by a separate catalytic Raf molecule in *trans*.

To understand how KSR regulates Raf-dependent MEK activation[6,7], we determined the crystal structure of the KSR2(KD)–MEK1 complex (Fig. 1 and Supplementary Table 1). KSR2(KD)–MEK1 dimers assemble into a tetramer through a KSR2(KD) homodimer interface centred on Arg 718 (Supplementary Fig. 1a). In solution, KSR2(KD)–MEK1 tetramers and dimers exist in dynamic exchange, indicating a relatively weak KSR2(KD) homodimer interaction (Supplementary Fig. 1b). KSR2(KD) and MEK1 molecules interact with their catalytic sites facing each other through their activation segments and αG helices (Fig. 1 and Supplementary Fig. 2a), reminiscent of MEK[10] and Chk2 (ref. 11) homodimers (Supplementary Fig. 2b). MEK's activation segment, incorporating Raf phosphorylation sites Ser 218^{M} and Ser 222^{M} (where superscript M indicates MEK1), comprises a short α-helix connected to a segment of extended chain that forms an antiparallel β-sheet with the KSR2 activation segment (Fig. 1b). This mutually constrained interaction of the MEK1 and KSR2 activation segments is stabilized by contacts between non-polar residues. The structural similarity of MEK1 when in complex with KSR2 to isolated MEK1, including those bound to allosteric inhibitors[10,12,13] (Supplementary Fig. 3), indicates that MEK inhibitors engage a physiologically relevant conformation of the kinase.

MEK and KSR form constitutive complexes[14,15] stable to Raf phosphorylation[16,17], even though Ser 218^{M} and Ser 222^{M} phosphorylation would alter the conformation of the MEK1 activation segment. The integrity of the complex is probably conferred by the more extensive interface created by engagement of their respective αG helices (Fig. 1a, c). This is consistent with studies showing that mutation of MEK within a conserved hydrophobic motif (Met 308^{M} to Ile 310^{M}), contiguous with the αG helix, disrupts MEK–KSR1 interactions[17]. In the

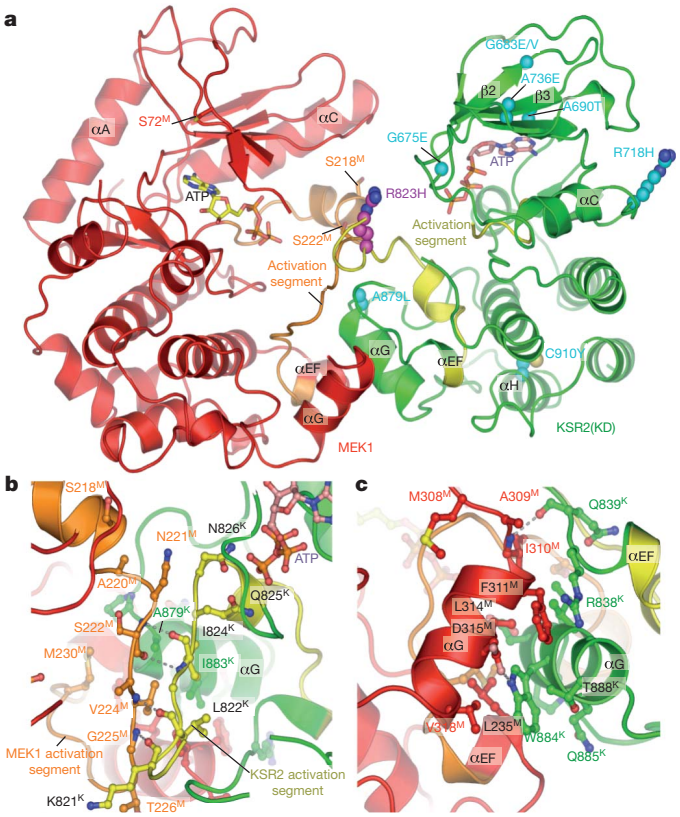

Figure 1 | Structure of the KSR2(KD)–MEK1 heterodimer. **a**, Overall view of the complex showing the face-to-face configuration of KSR2 and MEK1. KSR loss-of-function mutations[1–3] are shown with C atoms in cyan. A lung adenocarcinoma-associated mutation of KSR2 (R823H)[28] is located on the KSR2 activation segment interacting with the MEK1 activation segment. Sites of MEK1 phosphorylation (Ser 72, 218 and 222) are indicated. **b**, Details of the β-sheet formed between the activation segments of MEK1 and KSR2. **c**, Details of αG helix contacts.

[1]Section of Structural Biology, Institute of Cancer Research, Chester Beatty Laboratories, 237 Fulham Road, London SW3 6JB, UK. [2]Howard Hughes Medical Institute and Department of Cellular and Molecular Pharmacology, University of California San Francisco, San Francisco, California 94107, USA. [3]Department of Pharmaceutical Chemistry, University of California San Francisco, San Francisco, California 94107, USA.
*These authors contributed equally to this work.

complex, Ala 309^{M} and Ile 310^{M} contact KSR2 directly, whereas Met 308^{M} helps define the conformation of the αG helix (Fig. 1c). Furthermore, the KSR2(KD)–MEK1 structure rationalizes KSR genetic screens[2,16,18]. Tyr substitution of Cys 910^{K} (where superscript K indicates KSR2), a buried residue of the C-lobe αH helix, would destabilize the C-lobe, altering the αG helix conformation (Fig. 1a and Supplementary Fig. 4). In addition, replacement of Ala 879^{K} within the KSR2 αG helix with a bulky Leu residue in a KSR loss-of-function mutant[1] is not readily accommodated at the KSR–MEK interface (Fig. 1a, b), consistent with our finding that a KSR2(KD) A879L mutant destabilizes MEK1–KSR2(KD) interactions (Supplementary Fig. 5).

The KSR2(KD)–MEK1 crystal structure indicated that KSR has the potential for catalytic activity[19] possibly necessary for KSR function[6,20]. Electron density maps reveal well-defined density for ATP-Mg^{2+} at the KSR2(KD) catalytic site (Fig. 2a). Although Asp 803^{K} of the DFG motif is shifted slightly out of position, the metal-coordinating Asn 791^{K} and the general base Asp 786^{K} of the catalytic loop adopt conformations typical of conventional protein kinases (Fig. 2b). However, owing to the inactive position of its αC helix, reminiscent of inactive c-Src(KD) (refs 9, 21), KSR2(KD) adopts an inactive conformation (Supplementary Fig. 6). Conservation of ATP-binding-site residues, and the mapping of KSR loss-of-function mutants to the ATP pocket[2,3], indicate that ATP binding is necessary for KSR function (Fig. 1a and Supplementary Figs 4 and 7). A Thr substitution for Ala 690^{K} of β3, for example, would impede ATP binding, whereas a Glu substitution of Gly 675^{K} within the Gly-rich loop would disrupt the phosphate-binding site. Whereas *Drosophila* and *Caenorhabditis elegans* KSR share the same catalytic residues as conventional protein kinases, substitution of Arg for the conserved ATP-coordinating Lys residue in mammalian KSRs, the lack of reproducible kinase catalytic activity, and the capacity of kinase-impaired mutants of KSR to mediate MEK phosphorylation and MAP kinase signalling[16,22], have implicated KSR as a pseudokinase. Studies of pseudokinases such as HER3 indicate that functions other than catalysis are critical for their role in signal transduction cascades, and that their extremely low kinase activity may be sufficient to catalyse physiologically relevant transphosphorylation within a protein complex[23,24].

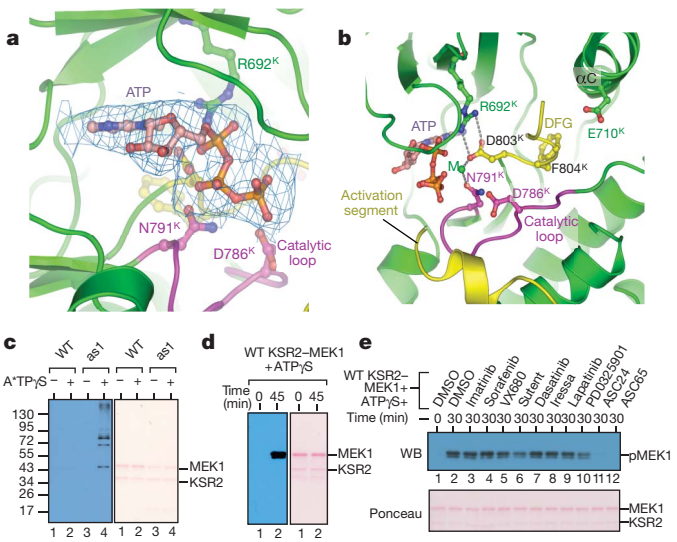

Figure 2 | KSR2 is a protein kinase. **a**, $2|F_o| - |F_c|$ electron density map for ATP bound to KSR2. **b**, Details of the catalytic site of KSR2. M, metal ion. **c**, Wild-type (WT) and T739G KSR (as1) KSR2–MEK1 complexes assayed in the presence of A*TPγS. Molecular mass markers in kDa are indicated along the left side of **c**. Phosphorylated proteins detected by western blot (WB) analysis (left) and total protein stained using ponceau red (right) are shown. **d**, Phosphorylation of MEK1 within wild-type KSR2–MEK1 combined with ATPγS. Phospho- (left) and total (right) proteins detected as in **c**. **e**, Enzymatic assay as in **d** in the presence of 10 μM of the listed inhibitors. Phospho-MEK1 is shown.

To examine putative KSR2 catalytic function we conducted *in vitro* kinase assays using an analogue-specific (as1) mutant of KSR2 (T739^{K}G) incubated with the modified ATP analogue N6-phenethyl ATPγS (A*TPγS). Resultant phosphorylation products include MEK1, specifically within the as1-KSR2(KD)–MEK1 complex (Fig. 2c, lane 4). MEK1 within the wild-type KSR2(KD)–MEK1 complex incubated with unmodified ATPγS was also reproducibly phosphorylated (Fig. 2d), an activity attributed to KSR2 because purified MEK1 does not autophosphorylate (Supplementary Fig. 8a).

To exclude further the possibility of MEK1 phosphorylation resulting from MEK1 autophosphorylation or by a contaminating kinase, we examined the influence of inhibitors in the KSR2(KD)–MEK1 assay (Fig. 2e and Supplementary Table 2). None of the compounds tested blocked 100% of the MEK1 phosphorylation reaction, including sorafenib, a Raf inhibitor, and PD0325901, a MEK inhibitor. Although the MEK1 inhibitors Sutent and PD0325901 blocked 50% of the reaction, other MEK1 inhibitors (VX680 and dasatinib) showed no inhibition. It is possible that Sutent and PD0325901 are binding to MEK1 and influencing its phosphorylation, an established feature of PD0325901 (ref. 25). The pan-protein kinase inhibitors ASC24 and ASC65 (ref. 26) block 100% of the activity in the KSR2(KD)–MEK1 kinase complex, indicating that KSR2 is a druggable target (Fig. 2e).

We next sought to identify the site(s) of phosphorylation in MEK1 catalysed by KSR2. We did not detect reactivity from activation segment phospho-specific antibodies (Ser 222^{M} and Ser 218^{M}/Ser 222^{M}) or for other MEK1 sites including Thr 286^{M} or Ser 298^{M} (data not shown). Using mass spectrometry, we identified Ser 24^{M} and Ser 72^{M} as KSR2-dependent phosphorylation sites in MEK1 not previously assigned to any known kinase (Supplementary Fig. 9a, b). KSR2 phosphorylates MEK1 with low discrimination because replacing Ser 24^{M} and Ser 72^{M} with alanines only reduced overall MEK1 phosphorylation by ~10% (Supplementary Fig. 8b). Additional KSR2-dependent sites were identified as Ser 18^{M} and Thr 23^{M} (Supplementary Fig. 9c). The stoichiometry of KSR2-catalysed MEK1 phosphorylation is 1.25% (data not shown), indicating a very inefficient reaction.

KSR assembles MEK–KSR–Raf ternary complexes responsible for promoting Raf phosphorylation of MEK[8,17,27] in which Raf interacts with the CA1 domain and CA5-kinase domain of KSR (refs 17, 27). The KSR2(KD) homodimer interface has a striking structural resemblance to the homodimer interface of BRAF(KD) (ref. 9), termed the side-to-side dimer interface and proposed to mediate Raf(KD)–KSR(KD) heterodimer interactions[8] (Fig. 3a, b). Both interfaces are centred on a conserved N-lobe Arg residue (Arg 718^{K} of KSR2 and Arg 509 of BRAF). Arg 718^{K} is functionally significant because its replacement with His, a loss-of-function mutation[2] (Fig. 1a), abolishes the capacity of Raf to activate MEK[8,22]. Notably, His substitution of Arg, shown to dissociate BRAF(KD) (ref. 8) and KSR2(KD) homodimers (Supplementary Fig. 10), would not be compatible with a Raf(KD)–KSR(KD) heterodimer. KSR2(KD) and BRAF(KD) homodimers adopt different quaternary modes (termed I and A, respectively), and only a subset of intersubunit contacts are common to KSR2(KD) and BRAF(KD) side-to-side dimer interfaces (Fig. 3 and Supplementary Figs 7 and 11). Raf phosphorylation of MEK is promoted by enforced dimerization of Raf and KSR kinase domains through the side-to-side dimer interface[8]. Conservation in KSR of BRAF side-to-side contact residues indicates that KSR and BRAF form heterodimers by means of the BRAF quaternary A mode.

The quaternary structure of the KSR2(KD)–BRAF(KD) heterodimer determines the tertiary structure of the KSR2 αC helix. An inactive conformation of the αC helix is incompatible with the BRAF quaternary A mode. Thus, formation of a KSR2–BRAF heterodimer (A mode) would be accompanied by a shift of the KSR2 αC helix to an active conformation (Supplementary Fig. 12), rationalizing the conservation of Phe 707^{K} and Glu 710^{K} of αC (Supplementary Figs 7 and 13). A

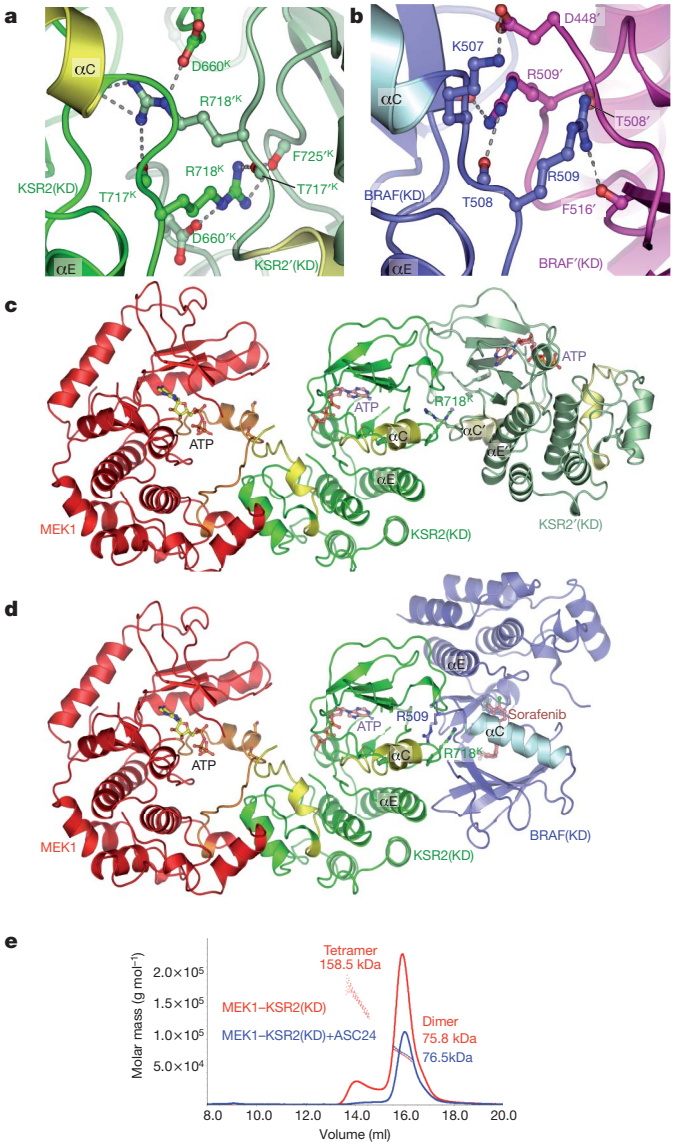

Figure 3 | KSR2 and BRAF homodimerize through a conserved side-to-side interface, but generate different quaternary structures. **a**, Details of the KSR2–KSR2 interface centred on Arg 718. Prime (′) denotes residues from the opposite subunit (quaternary mode I). **b**, Details of the BRAF–BRAF interface centred on Arg 509 (quaternary mode A) (Protein Data Bank 1uwh)[9]. **c**, MEK1–KSR2–KSR2 ternary complex. View as in Fig. 1a. **d**, Predicted MEK1–KSR2–BRAF ternary complex (quaternary mode A). **e**, Multiple angle laser light scattering experiment showing that ASC24 dissociates the KSR2(KD)–MEK1 heterotetramer into a heterodimer. The lower peak height in the presence of ASC24 is due to ASC24-induced protein precipitation.

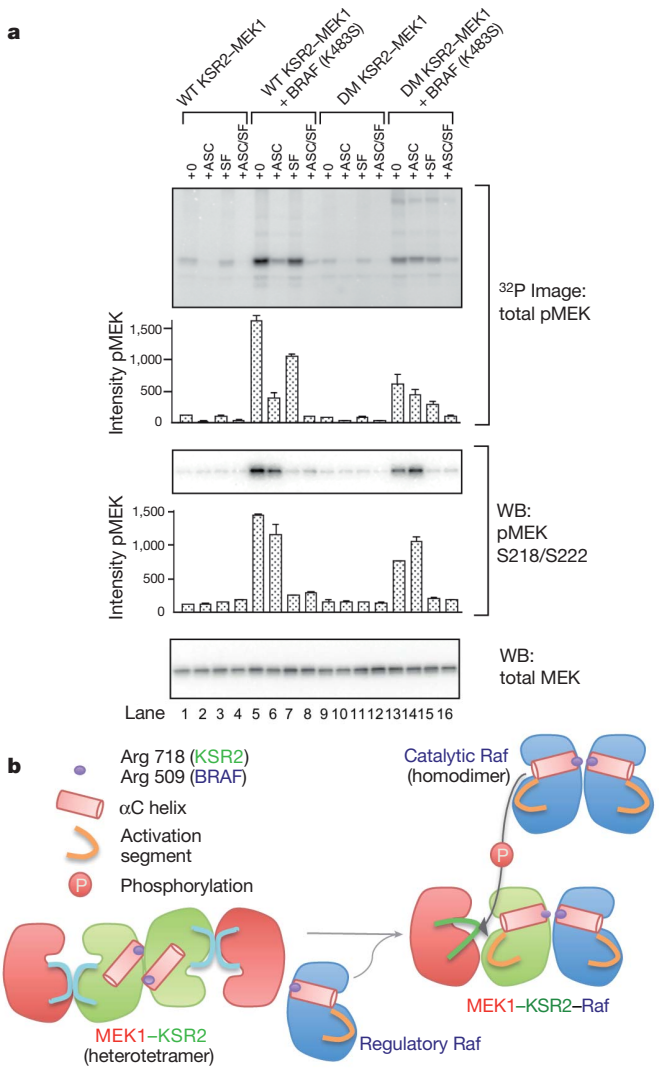

Figure 4 | Stimulation of MEK phosphorylation by an allosteric transition of KSR mediated by BRAF binding to the Arg 718 side-to-side interface. **a**, Biochemical reconstitution of KSR–Raf dimerization assessed based on MEK activation. Total phospho-MEK (top), S218/S222 site-specific phospho-MEK (middle), and total MEK (bottom; loading control) are shown. Bands were quantified and phospho-MEK levels were normalized relative to lane 1 in the top and middle panels, respectively. Error bars represent the mean ± s.d. ($n = 2$). **b**, Schematic of Raf-mediated activation of Raf phosphorylation of MEK. The side-to-side KSR2–Raf heterodimer (mode A) and Raf–Raf homodimer (mode A) are centred on Arg 718 (KSR2) and Arg 509 (BRAF). In the KSR2–MEK1 heterotetramer (left), the inaccessible activation segment of MEK1 is released through the interaction of KSR2 with a regulatory Raf molecule, induced by a conformational change of the αC helix, allowing catalytic Raf to phosphorylate MEK (right). The regulatory Raf molecule could be a catalytically impaired oncogenic mutant BRAF, whereas the catalytic Raf could also be Raf of a MEK1–KSR2–Raf ternary complex. Regulatory and catalytic Raf could be different isoforms (B-RAF or C-RAF). A Raf molecule bound to KSR through a side-to-side heterodimer interface is sterically unable to phosphorylate MEK in *cis*, an activity that therefore must be performed by a different Raf molecule.

BRAF-induced conformational shift of the KSR2 αC helix into the active position would probably enhance KSR2 kinase activity and influence its interaction with the activation segment of MEK, thereby affecting Raf's capacity to phosphorylate MEK. To test whether KSR2–BRAF heterodimerization stimulates KSR2 and BRAF-dependent MEK phosphorylation, we performed *in vitro* kinase assays. To overcome the weak and transient KSR2–BRAF interactions we immobilized His_6-tagged MEK1, KSR2 and BRAF onto Co^{2+} resin. As shown in Fig. 4a, the addition of kinase-impaired BRAF(K483S) to KSR2(KD)–MEK1 increases total MEK1 phosphorylation 15-fold (compare lanes 1 and 5). Interestingly, most of the increased activity comes from accelerated KSR2 catalytic function (as opposed to activity from additional BRAF). Approximately 70% of total MEK1 phosphorylation and less than 10% of S218/S222-specific activity was blocked by the KSR2 inhibitor ASC24 (Fig. 4a, lanes 5 and 6). Furthermore, most of the stimulated phosphorylation occurred at non-BRAF sites, as sorafenib only blocked 30% of total MEK1 phosphorylation but over 90% of the S218/S222-specific signal (Fig. 4a, lanes 5 and 7). Thus, KSR2 is the major kinase responsible for stimulated MEK1 phosphorylation in lane 5, and this occurs through a BRAF(K483S)-induced increase in KSR2 catalytic activity. That the R718H dimer interface mutation in KSR2 (KSR2(DM)–MEK) significantly reduced BRAF-induced stimulation indicates that KSR2 modulation by BRAF(K483S) depends primarily on the Arg 718-mediated

side-to-side interface of KSR2–BRAF heterodimers (Fig. 4a, compare lanes 5 and 13). In the absence of BRAF, the dimer mutation in KSR2 is functionally silent (Fig. 4a, compare lanes 1–4 and 9–12), indicating that wild-type and dimer mutant KSR2 are indistinguishable in a basal state.

Interestingly, BRAF(K483S) retained kinase activity (Supplementary Fig. 14); however, its intrinsic catalytic activity was not modulated through heterodimerization with KSR2. Indeed, with KSR2 inhibited by ASC24, MEK1 phosphorylation by BRAF(K483S) in wild-type and dimer mutant KSR2(KD)–MEK1 was approximately equal (Fig. 4a, lanes 6 and 14; middle panel). Thus, the twofold increase in MEK1 phosphorylation at the BRAF-specific sites, which were upregulated through KSR2–BRAF heterodimerization (lanes 5 and 13; middle panel), more likely resulted from a change in MEK1 structure coupled to allostery in KSR2 rather than an increase in intrinsic BRAF catalytic activity. KSR2(KD) heterodimerization with wild-type BRAF also stimulates BRAF-mediated MEK1 phosphorylation (Supplementary Fig. 15).

Control experiments excluded the possibility that either MEK1 autophosphorylation or contaminating kinases contribute to MEK1 phosphorylation (Supplementary Fig. 16). Thus, our data provide evidence for KSR2 as a protein kinase, stimulated by its interactions with BRAF. The physiological significance of KSR2 kinase activity awaits identification of its cellular substrate(s); however, its BRAF-triggered activation provides an *in vitro* barometer of a conformational change in KSR2. The kinase-independent function of KSR2 modulation of MEK1 is further borne out by the KSR2 inhibitor ASC24, which induces an unexpected increase in MEK1 phosphorylation by BRAF(K483S) (Fig. 4a, lanes 13 and 14; middle panel). Presumably, ASC24 induced a conformational change in KSR2 that partially mimics KSR Arg 718 side-to-side binding by BRAF, thus altering MEK1 and allowing for its increased phosphorylation, consistent with the capacity of ASC24 to disrupt the KSR2(KD) homodimer interface (Fig. 3e). Thus, a KSR inhibitor that binds to the KSR–MEK complex and antagonises the BRAF-induced allosteric switch could function analogously to the Ras suppressor: the KSR(R718H) mutation.

Here we reveal that KSR functions as an effector molecule, receiving a stimulatory signal from an activated regulatory Raf molecule and relaying this to modulate the accessibility of the MEK activation segment for phosphorylation by catalytic Raf (Fig. 4b). Our results highlight the complexity and adaptability of protein kinases, pseudokinases and scaffolding molecules to integrate signal transduction processes.

METHODS SUMMARY

Expression, purification and crystallization of KSR2–MEK1. *Homo sapiens* KSR2 kinase domain (KSR2(KD), residues 634–950) with an N-terminal His_6 tag was co-expressed with full-length MEK1 and the $p50^{Cdc37}$ Hsp90 co-chaperone in the baculovirus/Sf21 insect cell system. The KSR2(KD)–MEK1 complex was purified and crystallized as described in Methods. Crystal structure determination, mutagenesis, compound synthesis, enzyme assays, mass spectrometry and other procedures were performed as described in Methods.

Full Methods and any associated references are available in the online version of the paper at www.nature.com/nature.

Received 4 June 2010; accepted 20 January 2011.
Published online 27 March 2011.

1. Kornfeld, K., Hom, D. B. & Horvitz, H. R. The *ksr-1* gene encodes a novel protein kinase involved in Ras-mediated signaling in *C. elegans*. *Cell* **83,** 903–913 (1995).
2. Sundaram, M. & Han, M. The *C. elegans ksr-1* gene encodes a novel Raf-related kinase involved in Ras-mediated signal transduction. *Cell* **83,** 889–901 (1995).
3. Therrien, M. *et al.* KSR, a novel protein kinase required for RAS signal transduction. *Cell* **83,** 879–888 (1995).
4. Clapéron, A. & Therrien, M. KSR and CNK: two scaffolds regulating RAS-mediated RAF activation. *Oncogene* **26,** 3143–3158 (2007).
5. Kolch, W. Coordinating ERK/MAPK signalling through scaffolds and inhibitors. *Nature Rev. Mol. Cell Biol.* **6,** 827–837 (2005).
6. Therrien, M., Michaud, N. R., Rubin, G. M. & Morrison, D. K. KSR modulates signal propagation within the MAPK cascade. *Genes Dev.* **10,** 2684–2695 (1996).
7. Michaud, N. R. *et al.* KSR stimulates Raf-1 activity in a kinase-independent manner. *Proc. Natl Acad. Sci. USA* **94,** 12792–12796 (1997).
8. Rajakulendran, T., Sahmi, M., Lefrancois, M., Sicheri, F. & Therrien, M. A dimerization-dependent mechanism drives RAF catalytic activation. *Nature* **461,** 542–545 (2009).
9. Wan, P. T. *et al.* Mechanism of activation of the RAF-ERK signaling pathway by oncogenic mutations of B-RAF. *Cell* **116,** 855–867 (2004).
10. Ohren, J. F. *et al.* Structures of human MAP kinase kinase 1 (MEK1) and MEK2 describe novel noncompetitive kinase inhibition. *Nature Struct. Mol. Biol.* **11,** 1192–1197 (2004).
11. Cai, Z., Chehab, N. H. & Pavletich, N. P. Structure and activation mechanism of the CHK2 DNA damage checkpoint kinase. *Mol. Cell* **35,** 818–829 (2009).
12. Fischmann, T. O. *et al.* Crystal structures of MEK1 binary and ternary complexes with nucleotides and inhibitors. *Biochemistry* **48,** 2661–2674 (2009).
13. Iverson, C. *et al.* RDEA119/BAY 869766: a potent, selective, allosteric inhibitor of MEK1/2 for the treatment of cancer. *Cancer Res.* **69,** 6839–6847 (2009).
14. Denouel-Galy, A. *et al.* Murine Ksr interacts with MEK and inhibits Ras-induced transformation. *Curr. Biol.* **8,** 46–55 (1998).
15. Yu, W., Fantl, W. J., Harrowe, G. & Williams, L. T. Regulation of the MAP kinase pathway by mammalian Ksr through direct interaction with MEK and ERK. *Curr. Biol.* **8,** 56–64 (1998).
16. Stewart, S. *et al.* Kinase suppressor of Ras forms a multiprotein signaling complex and modulates MEK localization. *Mol. Cell. Biol.* **19,** 5523–5534 (1999).
17. McKay, M. M., Ritt, D. A. & Morrison, D. K. Signaling dynamics of the KSR1 scaffold complex. *Proc. Natl Acad. Sci. USA* **106,** 11022–11027 (2009).
18. Muller, J., Cacace, A. M., Lyons, W. E., McGill, C. B. & Morrison, D. K. Identification of B-KSR1, a novel brain-specific isoform of KSR1 that functions in neuronal signaling. *Mol. Cell. Biol.* **20,** 5529–5539 (2000).
19. Zhang, Y. *et al.* Kinase suppressor of Ras is ceramide-activated protein kinase. *Cell* **89,** 63–72 (1997).
20. Sugimoto, T., Stewart, S., Han, M. & Guan, K. L. The kinase suppressor of Ras (KSR) modulates growth factor and Ras signaling by uncoupling Elk-1 phosphorylation from MAP kinase activation. *EMBO J.* **17,** 1717–1727 (1998).
21. Xu, W., Harrison, S. C. & Eck, M. J. Three-dimensional structure of the tyrosine kinase c-Src. *Nature* **385,** 595–602 (1997).
22. Douziech, M., Sahmi, M., Laberge, G. & Therrien, M. A. KSR/CNK complex mediated by HYP, a novel SAM domain-containing protein, regulates RAS-dependent RAF activation in *Drosophila*. *Genes Dev.* **20,** 807–819 (2006).
23. Jura, N., Shan, Y., Cao, X., Shaw, D. E. & Kuriyan, J. Structural analysis of the catalytically inactive kinase domain of the human EGF receptor 3. *Proc. Natl Acad. Sci. USA* **106,** 21608–21613 (2009).
24. Shi, F., Telesco, S. E., Liu, Y., Radhakrishnan, R. & Lemmon, M. A. ErbB3/HER3 intracellular domain is competent to bind ATP and catalyze autophosphorylation. *Proc. Natl Acad. Sci. USA* **107,** 7692–7697 (2010).
25. Alessi, D. R., Cuenda, A., Cohen, P., Dudley, D. T. & Saltiel, A. R. PD 098059 is a specific inhibitor of the activation of mitogen-activated protein kinase kinase *in vitro* and *in vivo*. *J. Biol. Chem.* **270,** 27489–27494 (1995).
26. Statsuk, A. V. *et al.* Tuning a three-component reaction for trapping kinase substrate complexes. *J. Am. Chem. Soc.* **130,** 17568–17574 (2008).
27. Roy, F., Laberge, G., Douziech, M., Ferland-McCollough, D. & Therrien, M. KSR is a scaffold required for activation of the ERK/MAPK module. *Genes Dev.* **16,** 427–438 (2002).
28. Greenman, C. *et al.* Patterns of somatic mutation in human cancer genomes. *Nature* **446,** 153–158 (2007).

Supplementary Information is linked to the online version of the paper at www.nature.com/nature.

Acknowledgements This work was supported by a Cancer Research UK grant to D.B., ICR studentships to D.F.B. and W.C.H.C. and HHMI grant to K.M.S. We thank staff at the ESRF for help with data collection and K. Wood and V. Good for help with protein production and Z. Zhang for assistance with cloning. Mass spectrometry was made possible by NIH grants NCRR RR015804 and NCRR RR001614. The MEK1/$p50^{Cdc37}$ baculovirus was a gift from C. Vaughan. We thank Cell Signaling Technologies for help with phosphospecific MEK antibodies.

Author Contributions D.F.B. determined and analysed the MEK1–KSR2 structure; A.C.D. conducted biochemical analysis of Raf–KSR–MEK phosphorylation and inhibitor studies; N.T.H. carried out phosphoproteomics mass spectrometry studies; W.C.H.C. helped with protein production; A.L.B. analysed mass spectrometry data; K.M.S. designed and analysed experiments relating to the Raf–KSR–MEK phosphorylation and inhibitor studies; and D.B. designed experiments and analysed data.

Author Information Coordinates and structure factors have been deposited in the RCSB Protein Data Bank with accession numbers 2y4i and 2y4isf, respectively. Reprints and permissions information is available at www.nature.com/reprints. The authors declare no competing financial interests. Readers are welcome to comment on the online version of this article at www.nature.com/nature. Correspondence and requests for materials should be addressed to D.B. (david.barford@ic.ac.uk) or K.M.S. (shokat@cmp.ucsf.edu).

METHODS

Cloning, expression and purification of KSR2(KD)–MEK1. A variety of KSR isoforms were screened for expression and crystallization. *Homo sapiens* KSR2 kinase domain (KSR2(KD), residues 634–950) with an N-terminal His_6 tag was co-expressed with full-length rabbit MEK1 (with 3C Precission-cleavable His_6 tag) and the $p50^{Cdc37}$ Hsp90 co-chaperone in the baculovirus/Sf21 insect cell system (a gift from C. Vaughan). KSR2(KD)–MEK1 was purified using Co^{2+}-Talon resin (Clontech) and incubated with GST-tagged Rhinovirus 3C Precission and λ-phosphatase overnight. The protein was then applied to a RESOURCE S column (GE Healthcare) connected to a 5-ml GST column (GE Healthcare) to trap 3C protease. Free MEK1 was either present in the flow through or eluted early. The KSR2(KD)–MEK1 complex eluted as a later peak. Uncleaved protein and λ-phosphatase were removed using Talon resin and the KSR2(KD)–MEK1 complex was applied to a HiPrep 16/60 Superdex 200 gel filtration chromatography column. KSR2(KD)–MEK1 eluted as two peaks, which according to multiple angle light scattering (MALS) corresponded to a heterotetramer and a heterodimer. A smaller third peak is often seen that corresponded to MEK1. Sequential gel filtration has shown that the heterodimer and heterotetramer are dynamic species and so these peaks were pooled. Size exclusion chromatography was performed on mutant KSR2(KD)(R718H)–MEK1 complexes as for wild-type protein.

Crystallization of KSR2(KD)–MEK1. The complex was concentrated to 10 mg ml^{-1} and incubated with 5 mM Mg-ATP. Aggregation was cleared by filtration or by centrifugation for 20 min at 4 °C at 16,000*g*. Sitting-drop crystallization trials were set up using a Phoenix robot (Art Robbins Instruments) at 4 °C, 14 °C and 20 °C using a variety of commercial screens. Inclusion of 10 mM Pr acetate increased crystal size. Thousands of crystal growth conditions were trialled and in excess of 80 crystals were tested for diffraction. This led to a KSR2(KD)–MEK1 data set with Mg-ATP co-crystallization to 3.8 Å resolution from a crystal grown at 20 °C in 12% (w/v) PEG 3350, 0.2 M Na citrate, 10 mM Pr acetate, Bis-Tris propane pH 6.25. A data set to 3.45 Å was subsequently collected, which was also from a Mg-ATP co-crystallization in a similar condition with Mg acetate in place of Pr acetate. Crystallographic data were collected at beam line ID 14.4 ESRF, Grenoble and processed using MOSFLM and the CCP4 Program suite[29].

KSR2(KD)–MEK1 structure determination. BRAF shares ~30% sequence identity with the KSR kinase domain. A systematic approach to solving the structure by molecular replacement was undertaken. The CaspR automated molecular replacement server (http://www.igs.cnrs-mrs.fr/Caspr2/) was used[30] and is an automated molecular replacement pipeline that generates multiple sequence alignments using TCoffee[31], before homology model building with MODELLER[32], molecular replacement with AMoRe[29] and model refinement based on CNS[33]. Multiple CaspR runs were performed using all the potential space groups, with data scaled with a 5 Å high-resolution cutoff as well as a 3.8 Å resolution cutoff with both available structures of MEK (Protein Data Bank 1s9j and 2p55) as well as structures of BRAF (Protein Data Bank 1uwh and 3c4c) and with tyrosine kinases. This strategy led to a correct molecular replacement solution found using MEK and a MODELLER produced homology model of KSR based on the N-terminal lobe of BRAF and the C-terminal lobe of ephrin tyrosine kinase. Tyrosine kinases were suggested as search models despite having 15–20% sequence identity by GenTHREADER[34]. Molecular replacement was used to solve the 3.45 Å data set.

SeMet anomalous difference maps. To obtain independent phase information, we obtained anomalous diffraction data from SeMet incorporated KSR2(KD)–MEK1 crystals. SeMet-labelled KSR2(KD)–MEK1 was prepared in the insect cell system using a procedure modified from ref. 35. Peak data sets were collected for two crystals, although the best of these only diffracted to 7 Å. Anomalous difference maps were useful for confirming the location of Met residues and thus the chain trace of KSR2(KD).

Mutagenesis of BRAF(KD) and KSR2(KD)–MEK1. Point mutations of BRAF kinase-impaired (K483S), gate-keeper KSR2(KD)(T739G) and dimer mutant KSR2(KD)(R718H) were introduced using standard procedures. BRAF mutant and human $p50^{Cdc37}$ were cloned pairwise into a modified pFBDM vector (Z. Zhang). An N-terminally His_8-tagged human KSR2 kinase domain (634–950) was mutated to generate a dimerization-impaired mutant (R718H) in the modified pFBDM vector. In addition the following KSR2(KD) mutants were prepared: (1) dimer mutant KSR2(KD)(R718H); and (2) KSR2 kinase-impaired mutant (catalytic Asp) KSR2(KD)(D786A). Gene-containing pFBDM vectors were converted into bacmids for baculoviral productions. The kinase-dead MEK1 mutant was Lys 97 to Met, and a double phosphosite mutant Ser 24 and Ser 72 to Ala was prepared.

BRAF kinase domain purification. Viruses of BRAF mutants were used to infect Sf9 cells at a multiplicity of infection of 2. Cell pellets were harvested after 3 days of expression. BRAF was expressed and purified according to ref. 9 with minor modifications. Mutant proteins were purified with Talon metal ion affinity and ion-exchange chromatography.

MALS analysis of the KSR2(KD)–MEK1 complex. We used multiple angle laser light scattering at 658 nm using a Dawn Heleos light scattering instrument (Eldan) attached to a UV detector of purified KSR2(KD)–MEK1 complex that was run at room temperature on a 24 ml Superose 6 analytical gel filtration column (GE Healthcare) at a rate of 0.5 ml min^{-1} by HPLC (Varian).

MALS analysis of the KSR2(KD)–MEK1 + ASC24 complex. MALS gel filtration purified KSR2(KD)–MEK1 was concentrated to 2 mg ml^{-1} before multiple angle laser light scattering (MALS) experiments. ASC24 was incubated with KSR2(KD)–MEK1 at a final concentration of 4.5 mM at 4 °C, before the MALS experiment. Protein samples were run at 20 °C on a 24-ml capacity Superdex 200 analytical gel filtration column (GE Healthcare) at a rate of 0.5 ml min^{-1} by HPLC (Varian). MALS were performed on the eluate at 658 nm using a Dawn Heleos light scattering instrument (Eldan) attached to a UV detector.

***In vitro* kinase assays.** Wild-type and mutant forms of KSR2(KD)–MEK1 used for kinase assays were purified as described for the KSR2(KD)–MEK1 used for crystallization, except that the cleavage and gel filtration steps were omitted. Coomassie-blue-stained SDS–PAGE gels of purified proteins are shown in Supplementary Fig. 18.

Thiophosphorylation experiment. For the thiophosphorylation kinase assays, approximately 1 μM of purified KSR2–MEK1 complex (wild type or the as1 mutant) was pre-incubated for 10 min in reactions containing 10 μM of the indicated small molecule drugs, 10 mM Tris 7.8, 10 mM $MgCl_2$ and 2% DMSO. Reactions were initiated by adding ATPγS or N6-phenethyl ATPγS (A*TPγS) as indicated and allowed to proceed for 30 min, before being terminated with EDTA (0.025 mM final concentration). Thiophosphorylated reaction products were alkylated by adding 1.5 μl of a freshly prepared DMSO solution containing 50 mM para-nitrobenzyl mesylate (PBNM) to the mixtures. After incubation at room temperature for minimally 40 min, SDS-load dye was added, and samples were applied to a 4–20% Tris-HCl gel for SDS–PAGE separation. Proteins were transferred to nitrocellulose membrane, and then in sequence stained with ponceau dye, washed, blocked with 5% milk TBST, and then blotted using a phosphorothioate-specific monoclonal antibody (antibody 51-8; 1:10,000 in 5% milk)[36]. After removal of excess primary antibody and several washes, the membranes were incubated with HRP-conjugated anti-rabbit IgG secondary antibody (1:10,000 in 5% milk; Promega). Membranes were washed extensively, after which protein bands were visualized on film using enhanced chemiluminescence (Pierce).

Compound synthesis. Sorafenib, ASC24 and ASC65 were synthesized as previously described[26,37]. All other kinase inhibitors were obtained from Calbiochem or commercially available sources. Drugs were dissolved in DMSO before use.

Kinase assays on Co^{2+}-Talon beads. To overcome the weak and transient KSR2–BRAF interactions we immobilized His_6-tagged MEK1, KSR2 and BRAF onto Co^{2+}-Talon resin. We used this simplified reconstituted system to promote BRAF dimerization with purified KSR2–MEK1 complexes, and investigated the influence of these interactions on MEK1 phosphorylation. 1 μM of purified KSR2(KD)–MEK1 complex (wild type or mutants) was premixed with BRAF and then loaded onto Co^{2+}-Talon beads (Clontech). Beads were prepared from 50% slurry by washing in water. 2.0 μl of beads were used per reaction (25 μl total volume). For reactions containing free MEK1 (recovered), MEK1 isolated as a by-product from the KSR2(KD)–MEK1 complex was used. Free MEK1 (recovered) contains trace levels of KSR2 as detected by mass spectrometry. Kinases were diluted in buffer containing 10 mM Tris 7.8, 10 mM $MgCl_2$, 2% DMSO and 20 μM inhibitors as indicated. Reactions were initiated by the addition of 200 μM cold ATP supplemented with 5 μCi γ^{32}P-ATP and reactions were incubated at room temperature. After 90 min, reaction samples were mixed with SDS load buffer, heated, and electrophoresed on a 4–20% Tris-HCl SDS gradient gel. Gels were fixed, dried and exposed to a Typhoon phospho-imager to obtain the total MEK1 phosphorylation signal or transferred to nitrocellulose membranes and blotted with pMEK1/2 S217/S221 (Cell Signaling; 1:10,000 in 5% BSA TBST) or total MEK1 (Cell Signaling; 1:10,000 in 5% BSA TBST). Radioactive gels were scanned on a Typhoon imager (GE Healthcare) and bands were quantified using ImageQuant (GE Healthcare). Chemiluminescent signal on western blots was captured on a high-resolution digital camera using the AlphaInnotech system for quantification of pMEK on S218/S222 as shown in Fig. 4a. Graphing and analysis was performed using the program Prism.

Phosphopeptide mapping by tandem mass spectrometry. To identify phosphorylation sites we either enriched for phosphopeptides (ATP-treated KSR2(KD)–MEK1), or ran the whole protein digest directly on the mass spectrometer (A*TPγS-treated KSR2(KD)–MEK1). Preparations of the indicated kinase reaction were digested as described previously to retain the phosphorylation or thiophosphorylation mark[38]. The digested peptides were then desalted by using a C_{18} OMIX 100 μl Zip Tip. The phosphopeptides were then enriched by IMAC enrichment on a TiO_2 column as done previously[39]. The thiophosphorylated samples were not enriched. The peptides were run on a nano-LC system before

analysis on both a QSTAR Elie and a LTQ Orbitrap. For both, peptides were separated via a 60 min LC run (0–32% acetonitrile 0.1% formic acid). Separation was achieved by reversed-phase chromatography on a 75 μm × 15 cm C18 column flowing at 350 nl min^{-1} applied directly to a LTQ Orbitrap or a QSTAR Elite. For the LTQ Orbitrap, the three most intense ions above 10,000 counts were selected for subsequent fragmentation and MS analysis. Three CID spectra and three ETD spectra (200 = activation energy) were acquired. For the QSTAR Elite, the two most intense multiply charged peaks from each MS spectra were selected for fragmentation by CID, and MS analysis in the TOF mass analyser. For both, a dynamic exclusion window was applied that prevented the same peak from being selected for 1 min. Peak lists were generated by PAVA (in-house LTQ Orbitrap data) or Mascot (QSTAR Elite data) and analysed on Protein Prospector (LTQ Orbitrap: parent mass tolerance, 20 p.p.m., fragment mass tolerance, 0.6 Da, three missed cleavages, max four modifications, no constant modifications, and phospho serine/threonine variable modifications) (QSTAR Elite same as above except: parent mass tolerance, 200 p.p.m., fragment mass tolerance, 300 p.p.m., thiophospho serine/threonine variable modification).

29. Collaborative Computer Project 4. The CCP4 suite: programs for protein crystallography. *Acta Crystallogr. D* **50,** 760–763 (1994).
30. Claude, J. B., Suhre, K., Notredame, C., Claverie, J. M. & Abergel, C. CaspR: a web server for automated molecular replacement using homology modelling. *Nucleic Acids Res.* **32,** W606–W609 (2004).
31. Poirot, O., Suhre, K., Abergel, C., O'Toole, E. & Notredame, C. 3DCoffee@igs: a web server for combining sequences and structures into a multiple sequence alignment, *Nucleic Acids Res.* **32,** W37–W40 (2004).
32. Sali, A. & Blundell, T. L. Comparative protein modelling by satisfaction of spatial restraints. *J. Mol. Biol.* **234,** 779–815 (1993).
33. Brünger, A. T. *et al.* Crystallography & NMR system: A new software suite for macromolecular structure determination. *Acta Crystallogr. D* **54,** 905–921 (1998).
34. McGuffin, L. J. & Jones, D. T. Improvement of the GenTHREADER method for genomic fold recognition. *Bioinformatics* **19,** 874–881 (2003).
35. Cronin, C. N., Lim, K. B. & Rogers, J. Production of selenomethionyl-derivatized proteins in baculovirus-infected insect cells. *Protein Sci.* **16,** 2023–2029 (2007).
36. Allen, J. J. *et al.* A semisynthetic epitope for kinase substrates. *Nature Methods* **4,** 511–516 (2007).
37. Bankston, D. *et al.* A scaleable synthesis of BAY 43-9006: A potent raf kinase inhibitor for the treatment of cancer. *Org. Process Res. Dev.* **6,** 777–781 (2002).
38. Hertz, N. T. *et al.* Chemical genetic approach for kinase-substrate mapping by covalent capture of thiophosphopeptides and analysis by mass spectrometry. *Curr. Prot. Chem. Biol.* **2,** 15–36 (2010).
39. Trinidad, J. C. *et al.* Quantitative analysis of synaptic phosphorylation and protein expression. *Mol. Cell. Proteomics* **7,** 684–696 (2008).